Modelling and LPV control of an electro-hydraulic servo system

Proceedings of the 2006 IEEE
International Conference on Control Applications
Munich, Germany, October 4-6, 2006

Modelling and LPV control of an electro-hydraulic servo system

Frans Wijnheijmer, Gerrit Naus, Wil Post,
Maarten Steinbuch and Piet Teerhuis

Abstract— **This paper aims to show the modelling and control of an hydraulic servo system, targeting at frequency domain based controller design and the implementation of a LPV controller. The actual set-up consists of a mass, moved by a hydraulic cylinder and an electro-hydraulic servo valve. A nonlinear parametric model of the system, a number of fitted linear black box models as well as a LPV model combining these fits have been determined. In discretization of the control strategies for implementation on a digital control system, a new discretization algorithm is derived for LPV structures. Simulations and experimental results indicate the potential benefits of a position dependent controller over a classical controller, but show the limitations as well.**

I. Introduction

The classical and commonly used approach in the control of electro-hydraulic servo systems is based on local linearisation of the nonlinear dynamics of the system [5], [11]. However such approach requires conservative controllers that sacrifice performance in favour of robustness. In order to handle the position dependent dynamics of a hydraulic system [13] and [12] propose an adaptive controller. However, they apply the adaptation in a situation where the model can be predicted on beforehand. A force-based control synthesis is proposed by [8] to come to a sort of dynamic feedback linearisation. Although the results are promising, this approach merely shifts the nonlinear dynamics to the force controller than really solve the problem. To be able to cope with the nonlinear dynamics, [7] applies backstepping. Utilizing a gain-scheduling control synthesis, a controller that has the capability to vary for changing parameters can be found. [4] uses such a synthesis, Linear Parameter Varying (LPV) control, to control an injection-moulding machine. LPV is based on a robust (i.e. $\mathcal{H}_\infty$) control synthesis to come to a gain scheduling controller with proven stability [6].

This paper discusses the modelling and control of an electro-hydraulic servo system comparing classical-, $\mathcal{H}_\infty$ and LPV control. First a nonlinear parametric model, i.e. white box model, of the system is derived (Section II-B). The resulting insight in the system characteristics is used in developing a number of linear black box models (Section II-C). This shows the position dependent natural frequency, limiting the performance of a global controller. To be able to cope with this changing characteristics of the system effectively, frequency domain based controller design is used, ultimately targeting at a gain scheduling approach. Using loop shaping techniques, a classical controller is developed combining position and pressure feedback to achieve position tracking (Section III-A) in the first place. As a comparison, a number of local and a global $\mathcal{H}_\infty$ controller are developed next (Section III-B). Finally a LPV controller is developed (Section III-C), whose implementation required the development of a new discretization algorithm (Section IV).

The authors are with the department of Mechanical Engineering, Control Systems Technology group of the Eindhoven University of Technology, Eindhoven, The Netherlands. E-mail: g.j.l.naus@tue.nl, f.p.wijnheijmer@gmail.com, w.j.a.e.m.post@tue.nl, m.steinbuch@tue.nl, p.c.teerhuis@tue.nl

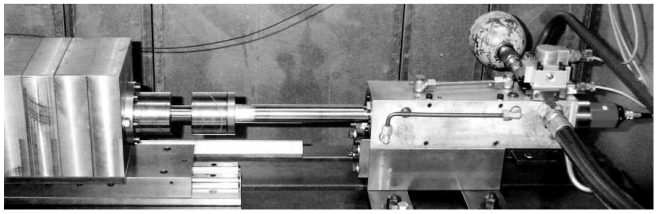

Fig. 1. The actual set-up of the electro-hydraulic servo system.

II. Modelling

A. System description

In our set-up the linear hydraulic actuator with hydrostatic bearings is mounted horizontally and drives a mass m. The weight of the mass is supported by a linear guide with rolling elements, so the friction is negligible. The actual hardware of the set-up is shown in Fig. 1 and the corresponding hydraulic diagram in Fig. 2. The electro-hydraulic servo valve used is a common four-way (symmetrical) critical center type of valve, but should be connected in a three-way valve configuration as in Fig. 2. Such configuration is necessary in case of asymmetric cylinders to avoid pressure jumps at the reversal of the movement of the rod, due to the difference in in- and out-going flows of the cylinder, see [11].

The servo valve is mounted on top of the cylinder to minimize the effects of the dead volumes. The position sensor is integrated in the piston rod of the cylinder and a pressure sensor for measuring the pressure in the piston chamber of the cylinder is mounted on the manifold of the servo valve. These sensors are assumed to be ideal and are not taken into account in the dynamic models. A current amplifier converting input voltage u to current i for the servo valve is also considered ideal.

0-7803-9796-7/06/$20.00 ©2006 IEEE

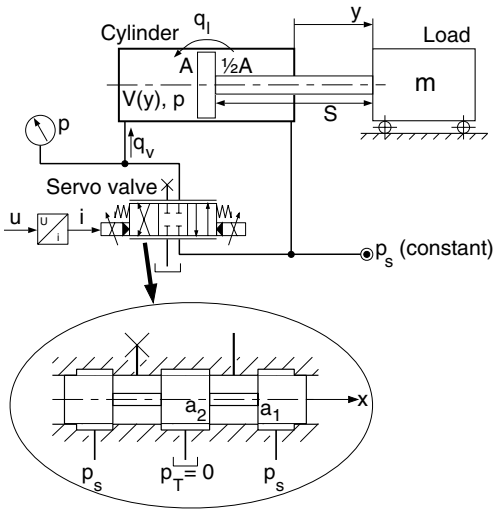

Fig. 2. Hydraulic diagram of the electro-hydraulic servo system.

B. White box model

In this section a parametric model of the system is derived, see Fig. 2. The load pressure is defined as $p_L = p - 1/2p_s$ and is normalized with respect to the supply pressure: $p_{Ln} = 2p_L/p_s \in [-1, 1]$. The leakage flow of the hydrostatic bearing is assumed to be laminar, i.e. linear with respect of the pressure difference across the narrow gap. Normalizing the leakage flow with respect to the maximum leakage flow q_{Ni}, i.e. the leakage flow at $p_{Ln} = -1$ results in: $q_l = 1/2q_{Ni}(1 - p_{Ln})$. From the mass balance of the piston side of the cylinder follows ([5], [11]):

$$A\dot{y} = -\frac{V}{E}\dot{p}_L + q_v + q_l \tag{1}$$

where A is the piston area, y is the position, V is the total trapped volume of the fluid, E is the effective bulk modulus and q_v is the valve flow. The total volume V equals $V = V_0 + Ay$. So the dynamics of the cylinder change during movement of the load, indicating nonlinear behaviour. Eq. (1) can be rewritten in the normalized form of:

$$\dot{p}_{Ln} = \frac{2E}{p_s V}\left(q_v - A\dot{y} + \frac{1}{2}q_{Ni}(1 - p_{Ln})\right) \tag{2}$$

The valve flow q_v is a nonlinear function of the pressure difference across the valve ports (a_1 or a_2) and the valve spool position x, see Fig. 2. The valve flow is assumed to be turbulent (orifice flow: $q = A_0(x)C_d\sqrt{\Delta p}$ [5]), so the volume flow for the critical center servo valve is given by:

$$\begin{array}{rclcl} q_v & = & c_0 x\sqrt{p_s - \frac{|x|}{x}p_L} & = & q_N x_n\sqrt{1 - \frac{|x_n|}{x_n}p_{Ln}} \\ c_0 & = & C_d w\sqrt{\frac{2}{\rho}} & & \end{array} \tag{3}$$

where q_N is the rated volume flow of the valve at full input signal (or $x = x_{max}$) and at $p_L = 0$ and is given by the manufacturer, $x_n = x/x_{max}$ is the normalized valve spool position , C_d is the effective discharge coefficient, w the width of the port of the valve and ρ is the density of the fluid.

Eq. (3) is linearized for small variations (x_e, p_e) around a working point $(x_0, p_0) = (\varepsilon, 0)$ of the servo valve, i.e. at no static load and at a small valve opening. The latter is a necessary condition for a turbulent flow, otherwise the flow becomes laminar, thus already linear in the valve spool position x. Linearisation of (3) results in:

$$q_v = q_{lin} = q_N\left(x_n - \frac{|x_n|}{x_n}\frac{\varepsilon}{2}p_{Ln}\right) \tag{4}$$

Because of the negligible friction the load dynamics reduce to:

$$m\ddot{y} = \frac{p_s}{2}Ap_{Ln} \tag{5}$$

where m is the total of the moving mass. Combining the dynamic models (2), (4) and (5) yields (see also [11]):

$$\frac{mV}{EA^2}\dddot{y} + \frac{m}{A^2 p_s}(q_{N_l} + q_N\varepsilon)\ddot{y} + \dot{y} = \frac{q_N}{A}x_n \tag{6}$$

The dynamics of the servo valve, i.e. of the first stage(s) should be considered. In this case, the valve has a substantial phase lag in the range of interest, influencing the system dynamics. Derived from the transfer function of the servo valve as provided by the manufacturer a second order system has been determined, see [10]. Taking into account the ideal dynamical behaviour of the current amplifier, the transfer function of input signal u (voltage) to valve spool position x_n can be given by:

$$\frac{X_n}{U} = \frac{1}{c_1 s^2 + c_2 s + 1} \tag{7}$$

where s is the Laplace operator, $c_1 = 1/\omega_{0,V}^2$ and $c_2 = 2\beta_V/\omega_{0,V}$, with β_V and $\omega_{0,V}$ the damping ratio respectively the natural frequency of the valve, are the constants resulting from fitting (7) on supplier data. For this servo valve a natural frequency of $f_{n,V} = 2\pi\,\omega_{0,V} \approx 120$ Hz is found. Attention is paid to fit on the phase rather then the amplitude characteristic, since the phase lag is most important in control design, see [3] and also section III.

Using a Laplace transformation, (6) is transformed into transfer functions for the position- and for the pressure responses respectively. In combination with (7), this yields:

$$\frac{Y}{U} = \frac{1}{(c_1 s^2 + c_2 s + 1)}\cdot\frac{c_3}{s(c_4 s^2 + c_5 s + 1)} \tag{8}$$

$$\frac{P_{Ln}}{U} = \frac{1}{(c_1 s^2 + c_2 s + 1)}\cdot\frac{c_6 c_3 s}{(c_4 s^2 + c_5 s + 1)} \tag{9}$$

with

$$\left\{\begin{array}{rcl} c_3 & = & \frac{q_N}{A} \\ c_4 & = & \frac{m}{EA^2}V = 1/\omega_0^2 \\ c_5 & = & \frac{m}{A^2 p_s}(q_{N_l} + q_N\varepsilon) = 2\beta/\omega_0 \\ c_6 & = & \frac{2m}{Ap_s} \\ V & = & Ay + V_0 \end{array}\right.$$

where ω_0 is the natural frequency of the system and β is the damping ratio of the system. Note that parameter c_4 is position (y) dependent, resulting in a shifting complex position-dependent pole pair in both the position and the

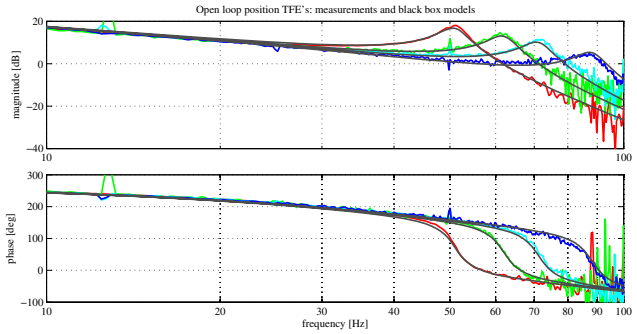

Fig. 3. Measured open loop position TFE's and the corresponding black box model transfer functions from u to y. From left to right, the plots correspond to a position of 95%, 50%, 25% and 5% of the stroke S respectively. The black box models are plotted on top of the measured TFE's.

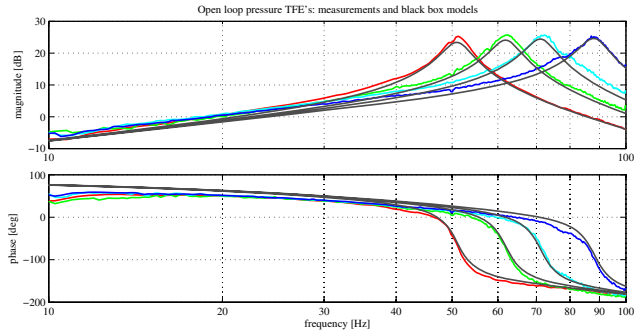

Fig. 4. Measured open loop pressure TFE's and the corresponding black box model transfer functions from u to p_L. From left to right, the plots correspond to a position of 95%, 50%, 25% and 5% of the stroke S respectively. The black box models are plotted on top of the TFE's.

pressure transfer function responses. Consequently (8) and (9) are only linear at fixed positions, resulting in a nonlinear parametric model. Furthermore the position transfer function response (8) has an integrating action, while the pressure transfer function response (9) has a differentiating action.

C. Black box model

Input -output measurements were performed on the experimental set-up in order to determine actual Transfer Function Estimates (TFE's) to validate the modelling. Based on the white box model of the system (Eq. (8), (9)), at different working points linear black box models are fitted on these TFE's using pole-zero placement techniques.
The white box models revealed one moving complex pole for different rod positions and two position independent poles describing the valve dynamics. Consequently a set of linear black box models for varying positions has been determined including separate models for the position and for the pressure. The black box models of the position transfer functions include an integrating action, identical poles for the valve dynamics (determined by $\omega_{0,V}$ and β_V) and a model specific complex pole pair at the natural frequency ω_0. The models of the pressure transfer functions include a differentiating action, the same fixed poles for the valve dynamics and the same model specific complex pole pairs.
The resulting black box models are plotted on top of the measured TFE's in Fig. 3 and 4. Note that the phase lag due to the servo valve dynamics indeed appears to be significant. As Fig 3, 4 demonstrate, the black box models are an accurate representation of the system at specific working points. Consequently these models will be used in further controller design.

D. LPV model

Anticipating at the development of a LPV controller (see Section III-C), a LPV model is derived. A LPV model in fact is a state-space model with parameters that are linear dependent on a variable (see [2]). In this case the position dependency of the system is taken into account by a variable θ. The white box model revealed a position dependency, which is approximately linear to $1/V$ (see Eq. (8), (9)). This yields for θ:

$$\begin{aligned} \theta &\approx \frac{1}{V} \sim \frac{1}{y} \\ &= \frac{1}{y + c_\theta} \end{aligned} \tag{10}$$

with c_θ a bias. After transformation of the black box models into a set of state-space models, the LPV model results from a linear least squares fit of these state-space models on the parameter θ:

$$\begin{cases} \dot{\underline{x}} &= A(\theta)\underline{x} + B\underline{u} \\ \underline{y} &= C\underline{x} + D\underline{u} \end{cases} \tag{11}$$

with $\underline{x}$ the state of the system and $\underline{u}$ and $\underline{y}$ the inputs respectively the outputs of the system. Validating figures, which are not included, show the good correspondence of the resulting LPV model with the black box models and the measurements.

III. Controller design

Modelling of the system shows the position dependent natural frequency. Considering controller design, this will limit the performance of a globally stable controller with respect to the performance of locally stable controllers. In order to cope with this changing characteristics of the system effectively, frequency domain based controller design is used, ultimately resulting in a gain scheduling approach. The models developed in Section II-C are used as a basis for controller design. To gain insight in the closed loop behaviour of the system, first a global classical controller is developed using loop shaping techniques. To value this design, which is mostly based on engineering skills, a $\mathcal{H}_\infty$ synthesis is used to design a global $\mathcal{H}_\infty$ controller. Next a LPV synthesis is used to develop a parameter varying controller, which has to include the possible benefits of a gain-scheduling approach, i.e. comprising the position dependency of the system in the controller. A number of local $\mathcal{H}_\infty$ controllers is designed to use as a benchmark for the resulting LPV controller. Frequency domain results are compared locally as well as globally for all controllers.

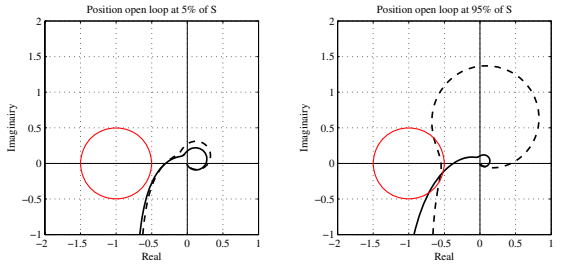

Fig. 5. Nyquist plots of the open loop system at 5% and at 95% of the stroke S (the left respectively the right figure). With respect to the dashed plots, pressure feedback is added to the open loop responses in the solid plots.

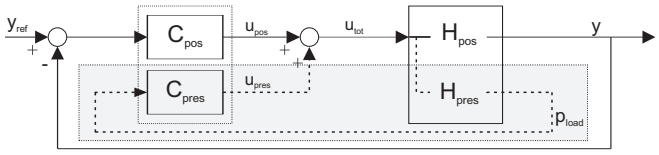

Fig. 6. Schematic layout of the closed loop position control system including pressure feedback.

A. *Classical feedback control*

The methods for designing classical feedback control of an electro-hydraulic servo system are for example described by [11]. In this case loop shaping techniques are applied, which is a relatively easy and fast method to design controllers enabling insight in the (linear) closed loop behaviour of the system (see [9]).

Nyquist plots of the system (Fig. 5) indicate that the phase at the natural frequency is over $180°$. This implies that the system is so-called phase-stabilised [3]. Adding a differentiating action would result in a cancelation of this phase-stabilisation. However, pressure feedback has a dampening effect on the position feedback loop as well, as is shown in Fig. 5 (see also [11]).

Hence, the favourable layout of the controlled system has been chosen as a combination of position- and pressure feedback (see Fig. 6). Sequential loop closing can be used for closing both feedback loops properly. The pressure loop influences the behaviour of the position loop, but not the other way around. So generally the pressure loop is closed first after which the position loop is closed, determining the final system performance.

Due to the dynamics of the servo valve, in practice the pressure loop becomes too sensitive for more retracted rod positions. Consequently application of pressure feedback is only utilizable for extended positions of the rod (see Fig. 5). Since the controller has to be globally stable (for all positions), application of the pressure feedback is omitted. Similarly, implementation of a dampening notch filter appeared not to be effective.

Consequently a classical, globally stable controller only comprises a proportional gain. The global controller performance is determined by a local controller designed at the most extended rod position at which the natural frequency of the system is lowest. This controller will also be stable for more retracted positions. The Nyquist stability criterion, comprising a gain as well as a phase margin, is used to select a proper gain for the controller.

The controller is implemented as an analogue- as well as a digital controller. In the actual set-up, a bandwidth of about 15 Hz is achieved. Taking into account the complete working range of the system (5% up to 95% of the stroke S), this clearly is a conservative controller for most of this range; using controllers which are locally tuned, bandwidths of 25 up to 30 Hz can be achieved (see Section III-B). However, these controllers are only locally stable.

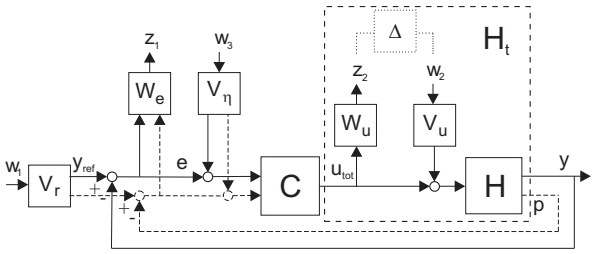

Fig. 7. General $\mathcal{H}_\infty$ system layout: the closed loop system including the $\mathcal{H}_\infty$ filters.

B. *$\mathcal{H}_\infty$ control*

$\mathcal{H}_\infty$ control can be regarded as a tuning method to make closed loop properties like the sensitivity (S) or the complementary sensitivity (T), meet criteria regarding performance and robustness of the controlled system. For this purpose, $\mathcal{H}_\infty$ input filters $V_{r,\eta,u}$ and output filters $W_{e,u}$ are added to the closed loop system (see Fig. 7). The shifting natural frequency has been modelled as a plant uncertainty Δ, which yields the position dependent plant H_t (see Fig. 7). The input-output relation for this so-called extended system then becomes:

$$\begin{pmatrix} z_1 \\ z_2 \end{pmatrix} = \begin{pmatrix} W_e S V_r & W_u C S V_r \\ W_e S P V_u & W_u T V_u \\ W_e T V_\eta & W_u C S V_{eta} \end{pmatrix}^T \begin{pmatrix} w_1 \\ w_2 \\ w_3 \end{pmatrix} \quad (12)$$

The closed loop properties S and T can now be shaped by the added filters, targeting at minimization of all input-output transfers $w_{1,2,3}$ to $z_{1,2}$ (see Eq. (12)). A theoretical description of $\mathcal{H}_\infty$ control is e.g. given by [6].

A $\mathcal{H}_\infty$ controller with reasonably good robust performance over the complete working range of the system could not be found. Consequently the final global $\mathcal{H}_\infty$ controller is only usable for positions between 50% and 95% of the stroke S. The controller has a bandwidth of about 10 Hz and shows a dip around the average natural frequency (see Fig. 8). In comparison to the classical controller this can be interpreted as a kind of skewed notch filter, which did not work for the global classical controller either.

In designing local $\mathcal{H}_\infty$ controllers (used to validate the LPV controller of Section III-C), the filters are adjusted to account for the plant uncertainty that can be decreased due

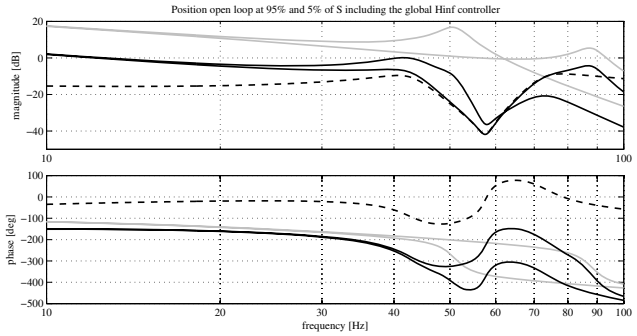

Fig. 8. Position open loop transfer functions of the system at 95% and at 5% of the stroke S (the solid dark plots) including the global $\mathcal{H}_\infty$ controller (the dashed plot). The solid grey plots show the corresponding black box models.

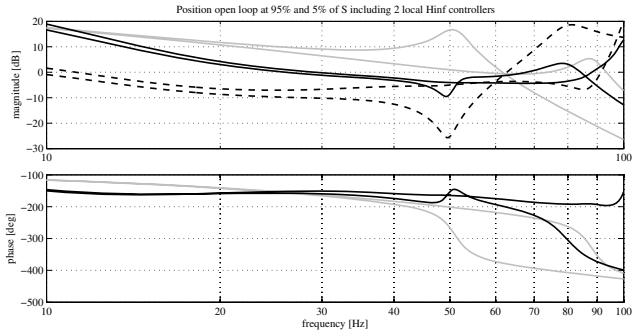

Fig. 9. Position open loop transfer functions of the system at 95% and at 5% of the stroke S (the solid dark plots) including two local $\mathcal{H}_\infty$ controllers (the dashed plots). The solid grey plots show the corresponding black box models.

to the smaller working range. The controllers are designed about the working points chosen in Section II-C (see Fig. 3). As a result a position dependent notch filter is present in the local $\mathcal{H}_\infty$ controllers. This yields an increased phase margin, which enables increasing of the gain of the controllers and thus increasing of the bandwidth of the controlled system of about 25 to 30 Hz (see Fig. 9).

C. LPV control

In the LPV synthesis used [1], the (non)linear dependency of the system on a varying parameter is taken into account in the controller design. As a varying parameter, θ is used (see section II-D) and the LPV model developed in Section II-D is used as a basis for the controller design. Hence the controller will be (linearly) dependent on θ. Although the achievable performance will change as a result of this, it should be able to achieve a global bandwidth and performance significantly better than those of the global $\mathcal{H}_\infty$ controller. Hence the controller structure of the local $\mathcal{H}_\infty$ controllers is used as a benchmark (see Section III-B). Unfortunately the resulting LPV controller does not incorporate a notch filter, which in fact made the local $\mathcal{H}_\infty$ controllers adaptive for different values of θ. This can be attributed to the robustness of the LPV controller for infinite fast changes in θ, which

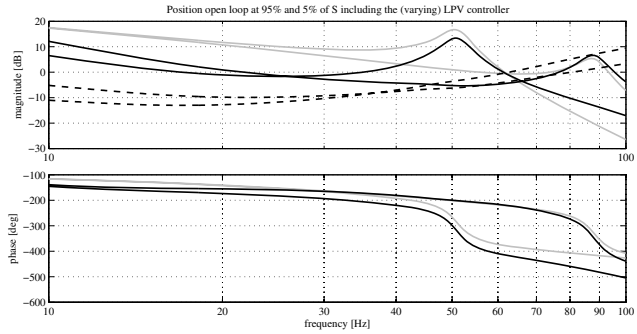

Fig. 10. Position open loop transfer functions of the system at 95% and at 5% of the stroke S (the solid dark plots) including the varying LPV controller (the dashed plots). The solid grey plots show the corresponding black box models.

is inherent to the LPV synthesis used. Consequently the resulting LPV controller is more conservative than necessary. Because of this, the performance of the LPV controller with a bandwidth of about 15 to 20 Hz is approximately identical to the performance of the global classical controller (see Fig. 9).

From this it may be concluded that the concept of the LPV controller appears to be appropriate, but the synthesis is too conservative. Syntheses with adjustable weights on the time derivative of the varying parameter θ are less conservative and could lead to results comparable to those of the locally tuned $\mathcal{H}_\infty$ controllers. However, the local $\mathcal{H}_\infty$ controllers contain a lot of nonlinear parameters with respect to θ, which makes e.g. combining of these controllers difficult. These syntheses are still under investigation.

IV. Implementation of the LPV controller

For actual implementation of the LPV controller, the controller has to be discretisized. However, standard discretization methods like a 1^{th}-order hold method perform a nonlinear transformation to the resulting system matrix. This would break up the LPV controller structure, which consists of two state-space systems. In literature no solution to this discretization problem could be found. In most cases an online discretization method is used or the analogue controller is implemented in a discrete manner. Consequently a new algorithm to transform the LPV controller to the discrete domain has been developed, such that transformations applied at the system matrices are performed on both state-space systems and no nonlinear transformations are made.

For a momentary value of θ, the corresponding state-space system is derived by a linear interpolation of the system matrices: the states are 'pulled out' of the system matrix and put into the feedbackloop $\dot{x} = \theta_1 \dot{x}_1 + \theta_2 \dot{x}_2$ with $\theta_1 = \theta$, $\theta_2 = 1 - \theta$ and the output $y = \theta_1 y_1 + \theta_2 y_2$ (see Eq. (13)). If this system is discretisized, the old states are not affected, because they have been 'pulled out' of the system into the C-matrix. The new A-matrix is also not affected, since it is a zero matrix that gives a unit matrix after discretization and

the resulting system becomes:

$$\left(\begin{array}{c} \dot{x}' \\ \hline \dot{x}_1 \\ \dot{x}_2 \\ y_1 \\ y_2 \end{array}\right) = \left(\begin{array}{c|cc} \emptyset & I & \emptyset \\ \hline A_1 & \emptyset & B_1 \\ A_2 & \emptyset & B_2 \\ C_1 & \emptyset & D_1 \\ C_2 & \emptyset & D_2 \end{array}\right) \left(\begin{array}{c} x' \\ \hline \dot{x} \\ u \end{array}\right) \tag{13}$$

Discretisizing this system (including the feedback loop) yields a system with a nonzero D-matrix. Combined with the static feedback loop, this results in an algebraic loop (originating from B_1 and B_2 in (13)). This loop can be solved for varying parameter θ, which results in a feedback loop with $x = x(u, x', \theta, \theta^2) + h.o.t.$. Neglecting the higher order terms, this can then be rewritten as a state space representation, which yields:

$$\left(\begin{array}{c} x'_{k+1} \\ \hline x_{1_k} \\ x_{2_k} \\ x_{3_k} \\ y_{1_k} \\ y_{2_k} \end{array}\right) = \left(\begin{array}{c|cc} I & I & \emptyset \\ \hline H_0 & \emptyset & K_0 \\ \theta_1 H_1 & \emptyset & \theta_1 K_1 \\ \theta_1^2 H_2 & \emptyset & \theta_1^2 K_2 \\ \theta_1 C_3 & \theta_1 D_{31} & \theta_1 D_{32} \\ \theta_2 C_4 & \theta_2 D_{41} & \theta_2 D_{42} \end{array}\right) \left(\begin{array}{c} x'_k \\ \hline x_k \\ u_k \end{array}\right) \tag{14}$$

The system of Eq. (14) has no algebraic loops and has been implemented successfully in the test set-up.

V. Conclusions and recommendations

A. Conclusions

Modelling: The parametric white box modelling provides good insight in the nonlinear characteristics of the system. Based on measurements and using this insight, a set of linear black box models is derived giving an accurate description of the system at several specific working points. The LPV model combines the accuracy of the black box models and the nonlinear system characteristics of the white box model.

Control: Global constant linear controllers like a classical or a $\mathcal{H}_\infty$ controller are limited in performance by the shifting natural frequency of the system. Damping the natural frequency by means of pressure feedback or implementation of a skewed notch is limited by the phase margin of the system, which is decreased in particular by the dynamics of the servo valve. As a result manual loop shaping techniques show slightly better results than a $\mathcal{H}_\infty$ synthesis.

Application of a LPV synthesis does not give rise to performance increase nor bandwidth increase of the resulting global controller comparable to the performances and bandwidths of local $\mathcal{H}_\infty$ controllers. Due to the inherent robustness of the LPV synthesis for infinite fast changes in (in this case) the position of the piston rod, the resulting controller is too conservative.

B. Recommendations

The concept of the LPV controller appears to be appropriate, but the synthesis is too conservative. Syntheses with adjustable weights on the time derivative of the varying parameter θ are less conservative and could lead to results comparable to those of the locally tuned $\mathcal{H}_\infty$ controllers. However, the local $\mathcal{H}_\infty$ controllers contain a lot of nonlinear parameters with respect to θ, which makes e.g. combining of these controllers difficult. These syntheses seem very promising.

References

[1] Apkarian P. and Gahinet P.; *A Linear Matrix Inequility Approach to H-infinity Control*, Int. J. of Robust and Nonlinear Control, Vol. 4, pp. 421–448, 1994.

[2] Apkarian P., Gahinet P. and Becker G.; *Self-scheduled Hinf Control of Linear Parameter-varying Systems: a Design Example*, J. of Automatica, Vol. 31, No. 9, pp. 1251–1261, 1995.

[3] Franklin G.F., Powell J.D. and Emani A.; *Feedback Control of Dynamic Systems*, John Wiley & Sons Inc., New York, USA, 1993.

[4] Matthijs Groot Wassink, Marc van de Wal, Carsten Scherer, Okko Bosgra; *LPV control for a wafer stage: beyond the theoretical solution*, Elsevier Control Engineering Practice, Vol. 13, No. 2, pp. 231–245, 2005.

[5] Merritt H.E.; *Hydraulic Control Systems*, John Wiley & Sons, Inc., New York, USA, 1967.

[6] Scherer C. and Weiland S.; *Linear Matrix Inequalities in Control*, Lecture Notes Disc Course on Linear Matrix inequalities in Control-2004/2005.

[7] Sirouspour M.R., Salcudean S.E.; *On the Nonlinear Control of Hydraulic Servo-systems*, Proc. ICRA '00, IEEE Int. Conf. on Robotics and Automation, Vol. 2, pp. 1276–1282, 2000.

[8] Sohl G.A., Bobrow J.E.; *Experiments and Simulations on the nonlinear Control of a Hydraulic Servosystem*, IEE Trans. on Control Systems Techn., Vol. 7, No. 2, pp. 238–247, 1999.

[9] Steinbuch M. and Norg M.L.; *Advanced motion control: and industrial perspective*, European J. of Control, No. 4, pp. 247–293, 1998.

[10] Thayer W.J.; *Transfer Functions for Moog Servovalves*, Moog Inc. Control Division, East Aurora, N.Y., Technical Bulletin 103, 1965.

[11] Viersma T.J.; *Analysis, Synthesis and Design of Hydraulic Servosystems and Pipelines*, Delft University of Technology, Dept. Mech. Eng., Delft, The Netherlands, Revised Edition, 1990.

[12] Yao B., Bu F., Chiu G.T.C.; *Non-linear adaptive robust control of electro-hydraulic systems driven by double-rod actuators*, Int. J. of Control, Vol. 74, No. 8, pp. 761–775, 2001.

[13] Yun J.S., Cho H.S.; *Adaptive model following control of electrohydraulic velocity control systems subjected to unknown disturbances*, IEE Proc., Vol. 135, Pt. D., No. 2, pp. 149–156, 1998.

Nomenclature

A	effective piston surface	$= 1.963\ 10^{-5}$	(m^2)
E	effective oil bulk modulus	$= 9\ 10^9$	(Pa)
S	stroke	$= 0.2$	(m)
V	total volume		(m^3)
V_0	dead volume		(m^3)
$f_{n,V}$	natural frequency of valve		(Hz)
i	input current		(A)
m	total mass	$= 130$	(kg)
p_L	load pressure		(Pa)
p_n	normalized pressure		
p_s	supply pressure	$= 7\ 10^6$	(Pa)
q_N	rated volume flow	$= 6.5\ 10^{-4}$	(m^3/s)
q_{N_l}	nominal leakage flow		(m^3/s)
u	input voltage		(V)
x	spool position of valve		(m)
x_n	normalized spool position		
y	position		(m)

Greek letters

β_V	damping ratio of the valve	
ε	linearisation point of x	
θ	LPV controller variable	
ω_0	natural frequency of system	(rad/s)
$\omega_{0,V}$	natural frequency of valve	(rad/s)